Simulation of Composite Tubes Axial Impact with a Damage Mechanics Based Composite Material Model

Xinran Xiao

General Motors Corporation, R&D Center
Warren, Michigan

Abstract

Composite tube axial impact is a benchmark problem measuring the predictive capability of composite crash simulation. A previous work revealed that MAT58 in LS-DYNA®, a continuum damage mechanics (CDM) composite material law based on Matzenmiller-Lubliner-Taylor (MLT) model, is inadequate in representing the unloading response of composite tubes that form continuous fronds in axial impact testing. To address the issue, two approaches have been attempted. The first one is to modify the compressive unloading response. The second one is to incorporate plasticity in a CDM framework. Both approaches were tested in an MLT theory based user material model. The modified MLT models improved the stability of the tube crush simulations and the simulation results.

1. Introduction

Fiber reinforced polymer composites offer high specific energy absorption (SEA) [1], which makes them attractive for energy absorbing applications such as front rails in vehicles, webbed fuselage structures, steering columns, and landing gears of helicopters. The high SEA of composites has not been fully utilized, and one of the key reasons is the lack of predictability.

Successful axial impact simulation cases have been reported for composite tubes. However, a close examination indicates that the success is related to the tube crush morphology. Figure 1 illustrates the three commonly observed crush zone morphologies in axial impact tests of composite tubes, denoted as Type I, Type II and Type III. Type I was classified as brittle fracturing [2] in which the material at the crush front broke into small debris. Type I is often observed in composite tubes reinforced with unidirectional prepreg [1-3], woven fabric [1,4] and chopped fiber [4]. In Type II, the material at the crush front did not break into small debris but formed continuous fronds. The fronds bent and rolled up the tube wall as crushing progressed. Type II is often observed in tubes reinforced with fabrics of large tow size such as braid, continuous strand glass mat (CSM) [5-7], and pultruded fiber glass [8]. Corner spitting is a unique energy absorption mechanism in this type of tubes. In Type III, the tube displayed an accordion liked folding pattern. Type III has been observed in tubes reinforced with Kevlar fibers [2,9]. These three crush morphologies were also reported for circular tubes under static crush load [2-3,9,10].

Composite tubes displaying Type I crush morphology have been successfully modeled by progressive damage models. Mamalis et al used MAT54 with LS-DYNA® to simulate carbon woven fabric/epoxy square tubes [11] and composite face sheets in composite tubes of sandwiched wall construction with a foam core [12]. By adjusting the TFAIL, a time step based element deletion parameter, and SOFT, a parameter that reduces the strength of the element

adjacent to the deleted element (assumed to be at the crush front), they were able to reproduce the load displacement traces and the crush morphologies. MAT 54 was also tested by Kim et al [13] for tubes reinforced with unidirectional fiber and by Makhecha [14] for tubes made of woven fabrics. Using RADIOSS®, Caliskan [15] demonstrated that a composite progressive failure model based on Tsai-Wu failure criterion (MAT25 of RADIOSS®) was able to reproduce the load-displacement traces of composite tubes with woven fabric reinforcement and to predict the crush load of the nose cone structure of a Jaguar F1 racing car.

For tubes displaying Type II crush morphology, the material in the crush zone moves away and forms continuous fronds instead of being crushed into debris. Braided composite tubes tend to form several continuous crush fronds which bend over or even roll up against the tube exterior wall [5,6]. The friction between the fronds and the impact platen [16,17] and the friction between the fronds and debris wedges [17] were considered as the major sources of energy absorption. The bending of the fronds itself also contributed to energy absorption [3,16]. Deleting elements that otherwise would form crush fronds will exclude these energy absorbing mechanisms in simulations. Our efforts using progressive failure models such as MAT54 were not able to produce stable simulations for braided composite tubes. On the other hand, steadily progress was made in this area using continuum damage mechanics (CDM) composite material laws. This paper provides a summary of the work in this area.

2. Tube Crush Experiment

Composite tubes were manufactured by a resin transfer molding process with 0/+30/-30 tri-axial braided carbon fiber reinforcement and vinyl ester resin. The tubes had 1-ply, 2-ply and 4-ply constructions. The mechanical properties of the composites are given in Table 1.

Composite tube axial crush experiments were performed using a free-flight drop tower [5], as shown in Figure 2. The total drop mass was 140 kg, and the drop height was 2.54 m. The measured initial velocity was 7.1 m/sec. The composite tubes were 360 mm in length. To ensure progressive failure, the impact end of the tube was chamfered with a 45º bevel. The tubes considered in this study had a square cross section of 55x55mm. Figure 2 gives an example of crush morphology of braided composite tubes.

Typical crush force-displacement curves obtained from braided composite tube axial crush experiments are shown in Figure 3. The total area under the force-displacement curve gives the measure of the energy absorption of the tube. This value is usually reported in terms of SEA.

3. CDM Framework

Following the notation of classic CDM [18-20], the modulus of elasticity of the undamaged material is denoted as E_0, the modulus of elasticity of the damaged material is denoted as E. The relationship between the two properties is

$$E = E_0(1-d) \qquad (3.1)$$

where d is a damage variable, $d \in [0,1]$. A damage value 0 to 1 corresponds to the undamaged state to a completely damaged state.

For an undamaged material, the stress-strain relation in the elastic range is given by the Hook's law

$$\sigma = \varepsilon E_0 \tag{3.2}$$

Where σ is the stress and ε is the strain. The elastic stress-strain relation for a damaged material is obtained from (3.1) and (3.2)

$$\sigma = \varepsilon E = \varepsilon E_0 (1-d) \tag{3.3}$$

Equation (2.3) indicates that the stress is always linearly proportional to the strain in terms of the elastic modulus of the damaged material. The stress-strain relation at any given point is uniquely determined if the elastic modulus of the damaged material is known.

In phenomenological CDM models, the damage variables are frequently expressed as functions of macroscopic measurable variables, such as strains [21], and generalized strains [22]. For example, an exponential damage evolution law as a function of strain was proposed in ref.21 as below

$$d = 1 - \exp\left[-\frac{1}{me}\left(\frac{\varepsilon}{\varepsilon_f}\right)^m \right] \tag{3.4}$$

where ε_f is the nominal failure strain, m is a parameter and e is the Naperian logarithm base.

The damage evolution described by Equation (3.4) is shown in Figure 4a. Figure 4b presents a 1-D stress-strain curve of a material described by Equation (3.3) with the damage law in Figure 4a. By representing the elastic modulus as a function of damage, the nonlinear stress-strain response including a post-peak softening behavior is generated with a linear stress-strain relation. This simple example illustrates the framework of the CDM constitutive models.

4. Simulations with CDM models

4.1 Experiences With MAT58

MAT58 in LS-DYNA® is based on a phenomenological CDM model proposed by Matzenmiller et al [21]. In a previous work [23], MAT58 was used for composite tube axial crush simulations. The multi-layered composite tubes were modeled with multi-layers of shell elements, and the shell layers were connected through tiebreak contact definition. Additional details regarding the FE models are in [23]. The results showed that the predicted peak crush forces were close to the experimental values but the predicted average crush forces were generally lower, particularly for the cases without a plug initiator. This also resulted in lower predictions for the SEA values.

To support the composite tube crush simulations, DeTeresa et al. [24] conducted tensile and compression experiments on braided composite coupons. They presented the stress-strain responses with softening behaviors that were not revealed in standard material characterizations. DeTeresa et al [24] also presented a stress-strain locus measured by a compression-tension load reversal experiment, as shown in Figure 5. Numerical simulation for the load reversal experiment was performed with MAT58 using one element. The numerical result is compared with the experimental curve in Figure 5. As seen, MAT58 is able to describe the monotonic loading segment rather well but not the unloading segment.

The discrepancy between MAT58 prediction and experimental results under a cyclic loading condition originates from the CDM framework. Attributing the nonlinearity and softening entirely to damage, a material described by a CDM model is always elastic and, therefore, follows a linear unloading path between the point of load reversal and the origin.

Improper representing unloading response can lead to error in energy absorption prediction. As seen, MAT58 predicted a much smaller area inside the stress-strain locus. The area enclosed in the stress-strain locus represents the irreversible energy absorption of the material. Under prediction of this energy absorption has two direct consequences. Firstly, it under predicts the total energy absorption of the structure. Secondly, it results in a greater amount of elastic energy release during unloading. Since the total energy is conserved in simulations, the released elastic energy adds oscillation and thus a greater tendency towards instability. It was suggested that improper modeling of the unloading response was a cause of the under-estimated crush force and SEA values using MAT58 as well as the great tendency to instability in tube axial crush simulations [23].

4.2 Simulations With CDM Models With Modified Unloading Path

4.2.1 UBC's CODAM Model
The suggestion about relationships between unloading response, instability and under-predicted SEA in composite tube crush simulations was examined in a subsequent work [25-27] using a user material model CODAM in LS-DYNA®. CODAM is a composite CMD model developed at the University of British Columbia (UBC) [22]. To better represent the compressively damaged materials, an analog model was developed and implemented in the CODAM model [25]. Simulations with the modified CODAM model generated more realistic crush morphologies and good correlation in terms of force-displacement responses and SEA values [27].

4.2.2 Modified MLT Model
Following the UBC's approach, a similar but simpler method was adopted to describe the compressively damaged materials [28]. It was implemented in a MLT model in the form of a user material model for LS-DYNA®.

The modified MLT model was tested in tube crush simulations for the case of a 2-ply, 0/+30/-30 tri-axial braided composite tube without a plug initiator. The simulation was relatively stable. Figure 6 compares the crush morphologies obtained from simulations using MAT58 and the modified MLT model. The crush fronds in the MAT58b simulation laid flat and the elements were distorted. The modified MLT model generated more realistic crush fronds.

The crush force-displacement response obtained by simulation is plotted in Figure 7, in comparison with the experimental result. The prediction of the average crush force and the total SEA value is improved when compared with the prediction with MAT58. Nevertheless, the values are still lower than the experimental results.

5. Simulations with A Coupled CDM-Plasticity Model

To represent post-peak softening and irreversible strains requires a coupled damage-plasticity model. Based on the physical evidence of damage accumulation process in composites and the

fundamentals of the two theories, a simple coupling method was proposed [29]. The capability of this method is examined by incorporating plasticity into the MLT model.

5.1 One element test

The coupled MLT-plasticity model was investigated using one element. The one-element model was subjected to a cyclic tensile loading under displacement controlled mode. Figure 8 displays the element strain history. As shown, the element is first subjected to tensile loading with a maximum strain of 0.015 and then unloading to a minimum strain of 0.003. At each subsequent cycle, the maximum strain increases but the minimum strain remains the same.

Figure 9 compares the stress-strain traces generated by simulations using the two material models. As expected, the unloading and reloading paths generated by MLT model follow the line from the point of load reversal to the origin. The trace generated by the coupled MLT-plasticity model is very different. Its first unloading path is similar to that of the MLT model because the unloading occurs before reaching the strain threshold, which is assigned a value equal to the strain at the peak stress. In the subsequent loading steps, the maximum strains are above the threshold and the contribution of plasticity is noticeable.

The compression-tension load reversal experiment as shown in Figure 4 was simulated under displacement controlled mode. Figures 10a and 10b present the stress-strain locus generated by simulations using the two material models. Due to the limitation in classic CDM discussed in section 4, the MLT model could not reproduce the locus as seen in experiments. The coupled MLT-plasticity model on the other hand can generate a locus resembling the experimental curve.

5.2 A composite tube subjected to axial impact

Simulations were carried out for a composite tube reinforced with 1-ply Fortafil 80k/80k 0/30/-30 braid. Figure 11 presents the deformation morphology at four different time frames generated in the simulation. As seen, the simulation was stable at all four time frames.

Figure 12 compares the force-displacement response generated in one of the simulations with the experimental curves. As shown, with a correlated material model, the peak force and the average force generated by simulation are in fairly good agreement with the experimental results.

6. Summary

Braided composite tubes form continuous fronds in axial impact testing. The material in fronds experiences unloading when moving out crush front. Correctly representing the stress-strain response in load reversal scenario is an important requirement in modeling the energy absorption in crash events. First, a modification to compressive unloading was proposed. Next, a coupled MLT-plasticity model was developed. These approaches were examined with a MLT model. The modified MLT model improved the stability of the tube crush simulations and the predictions on the average crush force and the SEA value.

7. Acknowledgements

8. References

1. Hull D, Energy Absorbing Composite Structures, Science and Technology Review, University of Wales 3, 23-30, 1988.
2. Farley GL. Effect Of Crushing Speed On Energy Absorption Capability Of Composite Tubes. J Compos Mater 1991, 25, 1314-1329.
3. Hamada H, Ramakrishna S, Comparison Of Static And Impact Energy Absorption Of Carbon Fiber/PEEK Composite Tubes, Composite Materials: Testing and Design, vol.12, ASTM STP 1274, RB Deo and CR Saff, Eds, American Society For Testing and Materials, 1996, 182-197.
4. Starbuck JM, private communications.
5. Johnson N, ACC Generic Tube Crush Program: Dynamic Crush Test of SRIM Tubes, Proceedings of the American Society for Composites 13th Technical Conference, Sept. 1998.
6. Johnson N, Browne AL, Houston D, Lalik L, ACC Generic Tube Crush Program: Comparison of Axial Crush of RTM and SRIM Tubes, Proceedings of the American Society for Composites 14th Technical Conference, pp. 641-650, Sept. 1999.
7. Thornton PH, Jeryan R, Crash Energy Management in Composite Automotive Structures, Int. J. Impact Eng., 7, 167-180, 1988.
8. Thornton PH, The crush behavior of pultruded tubes at high strain rates. J Compos Mater 1990, 24(6): 594-615.
9. Browne AL, Johnson N, Dynamic Axial Crush Test Of Roll Wrapped Composite Tubes: Tube Geometry and material Effects, Proceedings of the American Society for Composites 20th Technical Conference, 2005.
10. Chiu CH, Lu CK, Wu CM. Crushing Characteristics Of 3-D Braided Composite Square Tubes. J Compos Mater 1997, 31 (22):2309-2327.
11. Mamalis AG, Manolakos DE, Ioannidis MB, Papapostolou DP, The Static And Dynamic Axial Collapse of CFRP Square Tubes: Finite Element Modeling, Composite Structures, 2006, 74 (2): 213-235.
12. Mamalis AG, Manolakos DE, Ioannidis MB, Kostazos PK, Crushing Of Hybrid Square Sandwich Composite Vehicle Hollow Body shells With Reinforced Core Subjected To Axial Loading: Numerical Simulation, 2003, 61 (3):175-186.
13. Kim H, Ben G, Aoki Y, Impact Response Behavior of Rectangular CFRP Tubes for Front Side Members of Automobiles, 12th US-Japan Conference on Composite Materials, Dearborn, Michigan, September 2006.
14. Makhecha DP, Dynamic Fracture of Adhesively Bonded Composite Structures Using Cohesive Zone Models, PhD dissertation, Virginia Polytechnic Institute and State University, Blacksburg, VA, 2005.
15. Caliskan AG, Design & Analysis of Composite Impact Structures for Formula One Using Explicit FEA Techniques, Proceedings of the 2002 SAE Motorsports Engineering Conference and Exhibition, Indianapolis, Indiana, 2-5 December, 2002.
16. Brimhall TJ, Friction Energy Absorption In Fiber Reinforced Composites, Ph.D. Dissertation, Michigan state University, May 2005.
17. Fairfull AH, Hull D, Energy Absorption Of Polymer Matrix Composite Structures: Frictional Effected, Structural Failure, T Weirzbicki and N Jones, Eds., Wiley, New York, 1989, 255-279.
18. Krajcinovic, D. (1989), Damage Mechanics, Mechanics of Materials, 8:117-197.
19. Lamaitre, J. (1984), How to Use Damage Mechanics, Nuclear Engineering and Design, 80: 233-245.
20. Talreja, R. (1994), Damage Characterization By Internal Variables, Damage Mechanics of Composite Materials, R. Talreja, ed., Elsevier, Amsterdam.
21. Matzenmiller A, Lubliner J, Taylor RL, A Constitutive Model For Anisotropic Damage In Fiber-Composites, Mech. Mater, 1995; 20, 125-152
22. Williams KV, Vaziri R, and Poursartip A, A Physically Based Continuum Damage Mechanics Model for Thin Laminated Composite Structures, Int Journal of Solids and Structures, 40, 2003, 2267-2300.

23. Xiao X, Johnson N, Botkin M, Challenges In Composite Tube Crash Simulation, Proceedings of the American Society for Composites 18th Technical Conference, October 2003.
24. DeTeresa SJ, Allison LM, Cunningham BJ, Freeman DC, Saculla MD, Sanchez RJ and Winchester SW, Experimental Results In Support Of Simulating Progressive Crush In Carbon-Fiber Textile Composites, Lawrence Livermore National Laboratory, UCRL-ID-143287, 2001.
25. McGregor C, (2005), Simulation of Progressive Damage Development in Braided Composite Tubes Under Axial Compression, MASc. Thesis, Civil Engineering, The University of British Columbia.
26. Mcgregor C, Vaziri R., Poursartip A, Xiao X, Simulation Of Progressive damage Development In Braided Composite Tubes Under Axial Compression, Composites A. 38, 2007, 2247-2259.
27. Xiao, X., Mcgregor, C., Vaziri, R. and Poursartip, A. (2007), Progress In Composite Tube Crush Simulation, Proc of American Helicopter Society 63rd Forum, Virginia Beach, VA.
28. Xiao X, Modeling Energy Absorption With A Damage Mechanics Based Composite Material Model, J Composite Materials, accepted.
29. Xiao X, Modeling Energy Absorption Of Composite Structures With A Coupled Damage-Plasticity Model, to be presented at ASC 2008, Memphis, September 9-11, 2008.

Table 1 Mechanical Properties of 0/+30/-30 Tri-axial Braided Composite

Mechanical Properties	Ultimate Strength (MPa)	(Chord) Modulus (GPa)	Strain to Failure	Poisson's Ratio
0° tensile	305.4	42.3	0.0104	
90° tensile	32.1	5.7	0.0097	0.207
0° compression	120.7	32.2	0.0039	
90° compression	66.3	8.6	0.0085	
0° shear	86.2	9.0		
90° shear	82.1	8.8		

(a)   (b)   (c)
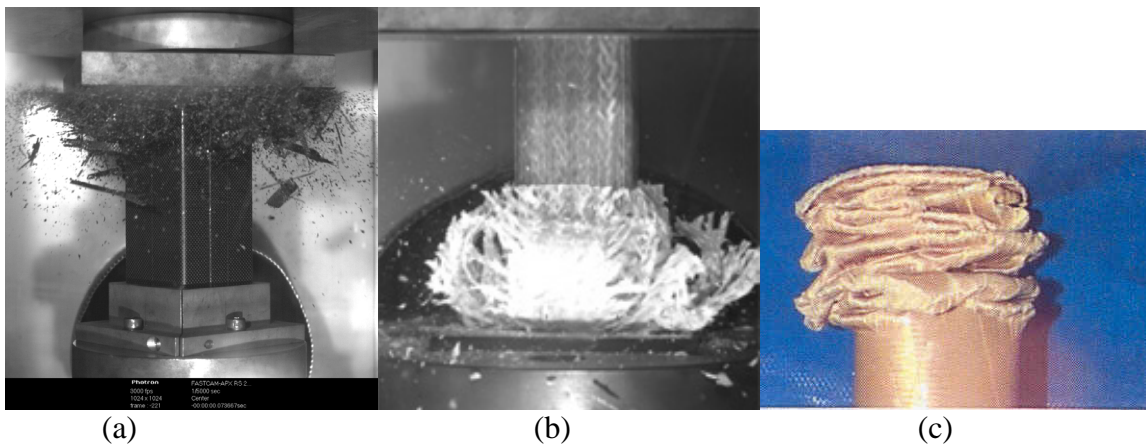
Figure 1   Three types of crushing morphology: (a) Type I - brittle fracture: as shown for a woven carbon fiber/epoxy tube [4]; (b) Type II - continuous fronds: as shown for a tri-axial braided carbon/vinyl ester composite tube [4]; (c) Type III - accordion folding: as shown for a Kevlar reinforced tube [9].

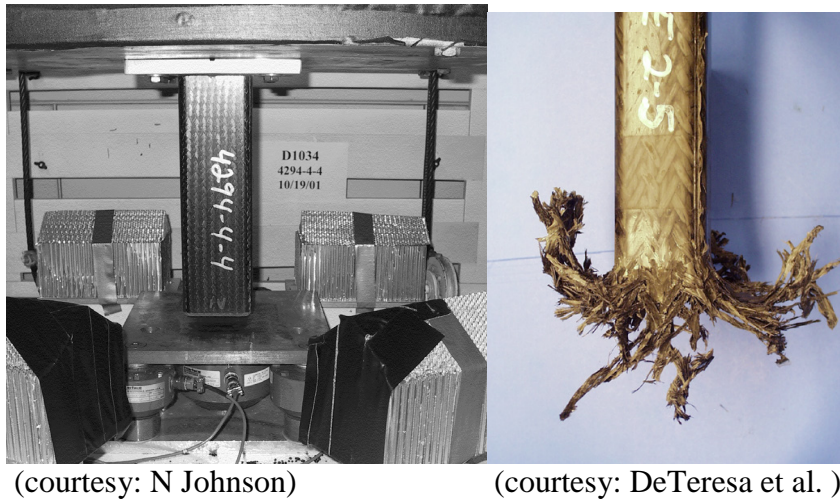(courtesy: N Johnson)   (courtesy: DeTeresa et al.)

Figure 2. Composite tube impact experiment set up and a tested tri-axial braided carbon fiber composite tube.
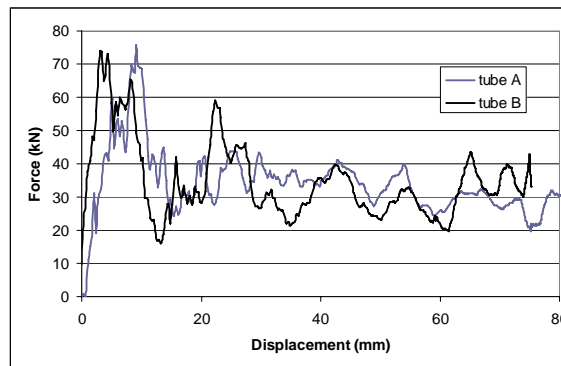

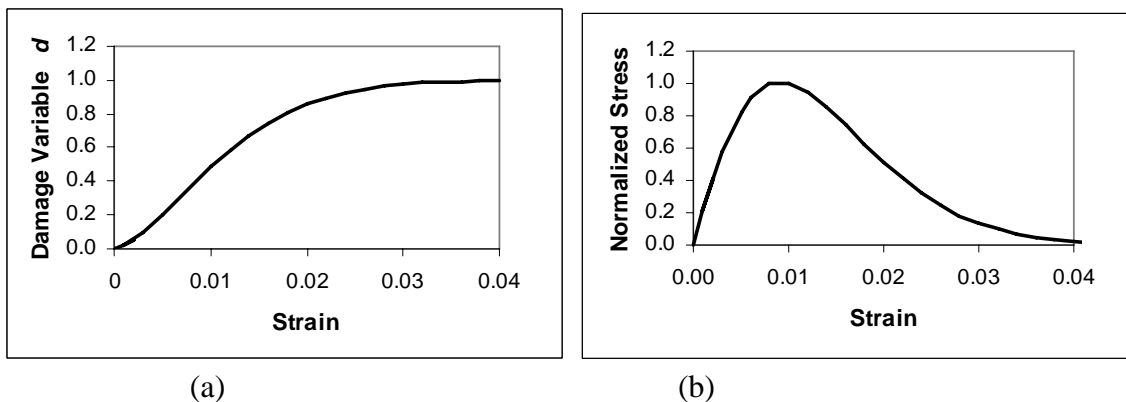Figure 3   Typical force-displacement responses of two identical braided composite tubes under axial crush.

(a)   (b)

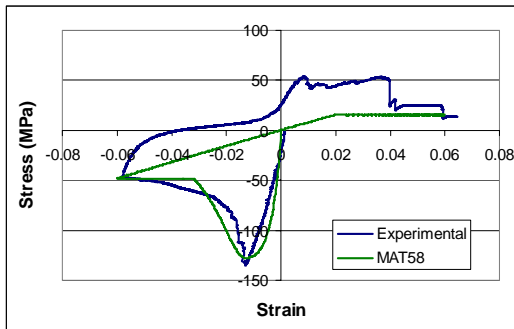Figure 4 (a) Damage evolution described by equation (2.4) and (b) the stress-strain curve produced by CDM.

Figure 5. Comparison of the stress-strain response of a MAT58b simulation to stress reversal experimental data of a 2-ply 0/±30 tri-axial braided composite. The specimen was loaded in compression, then unloaded and loaded to failure in tension. The experimental data was provided by DeTeresa [24].
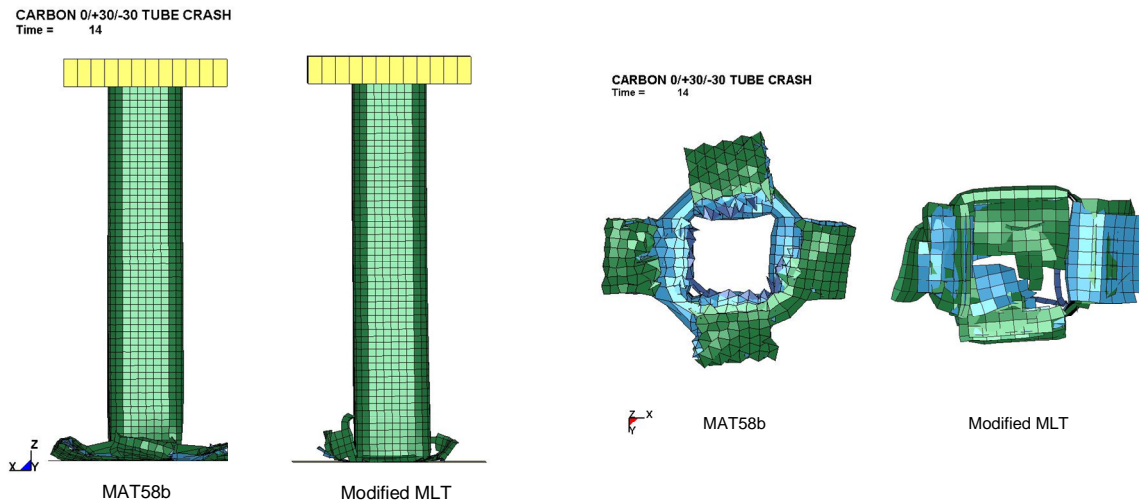
Figure 6. Simulations of a 2-ply 0/±30 tri-axial braided composite tube with MAT58b and MLT model with modified unloading path [28].
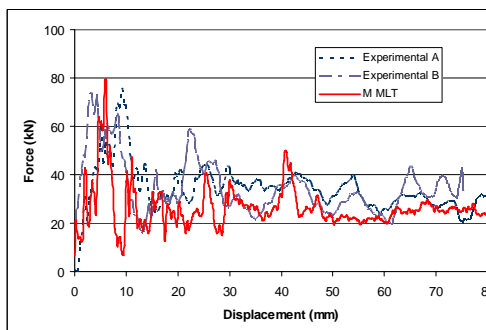
Figure 7. Comparison of experimental crush force-displacement responses with simulation using MLT model with modified unloading path [28]. The study was for the case of a 2-ply 0/±30 tri-axial braided composite tube without plug initiator.
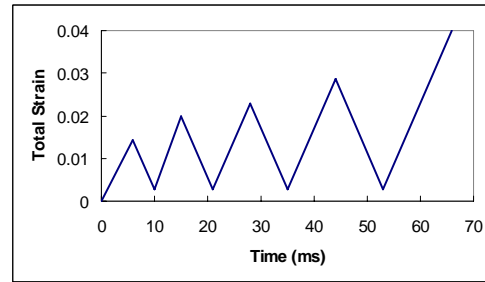

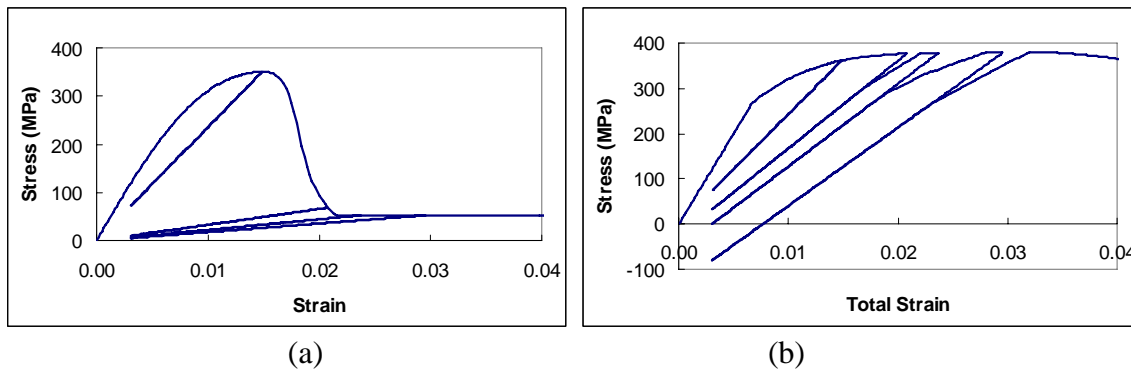Figure 8 The element strain history of a displacement controlled cyclic tensile experiment.

(a)   (b)

Figure 9 The element stress-strain locus generated by (a) the MLT model and (b) the coupled MLT-plasticity model [29] by simulations of the cyclic tensile experiment.

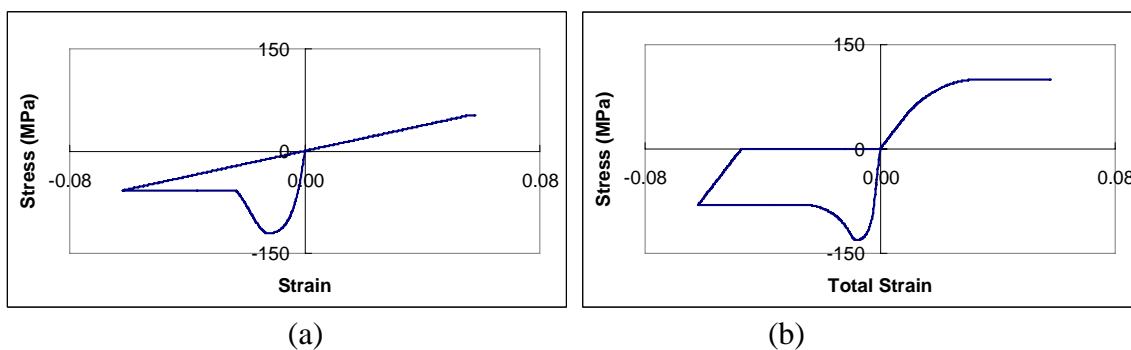(a)   (b)

Figure 10   Simulations of the compression-tension experiment. The stress-strain locus was generated by (a) the MLT model, (b) the coupled MLT-plasticity model [29].

Time =   4.9997   Time =   9.9999
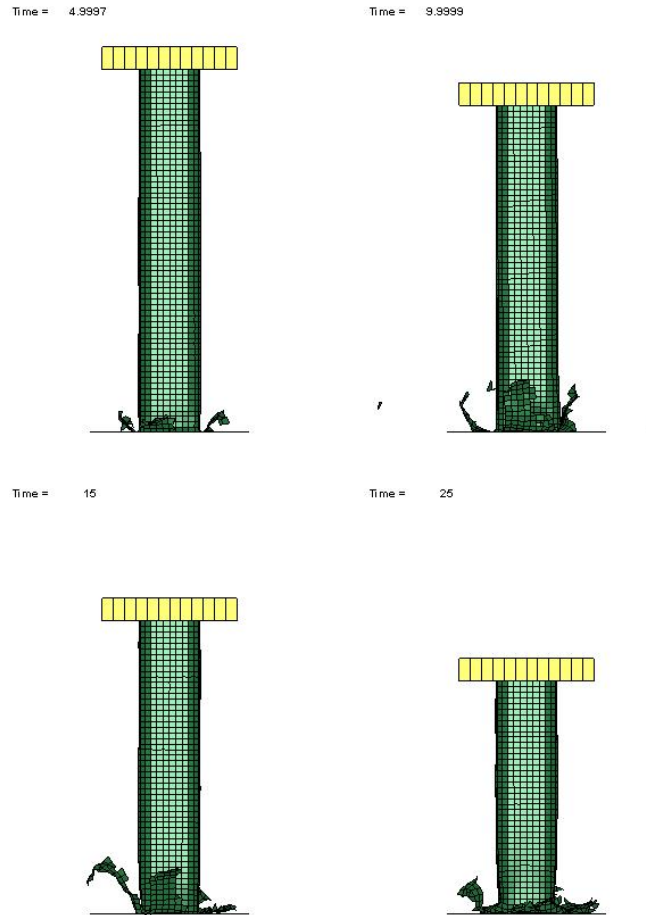
Time =   15   Time =   25

Figure 11 A composite tube reinforced with 1-ply tri-axial braid under axial impact. Simulation was performed using explicit FE code LS-DYNA® with the coupled MLT-plasticity model [29].
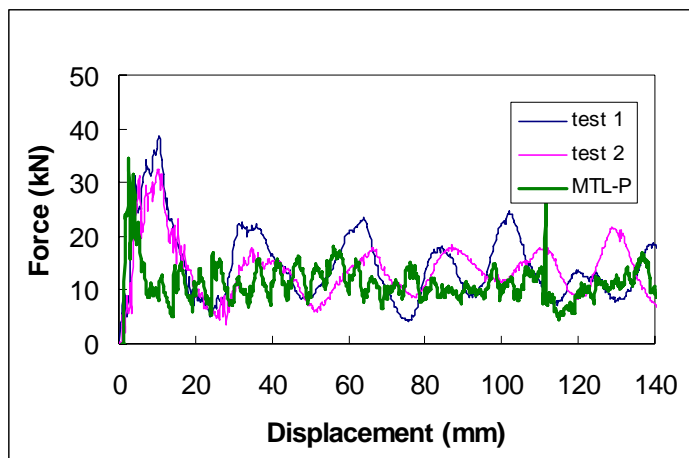
Figure 12 Comparison of force-displacement responses generated by simulation with experimental results for a composite tube reinforced with 1-ply tri-axial braid under axial impact.